β2 integrin mediates hantavirus-induced release of neutrophil extracellular traps

Martin J. Raftery,[1] Pritesh Lalwani,[1] Ellen Krautkrämer,[4] Thorsten Peters,[5] Karin Scharffetter-Kochanek,[5] Renate Krüger,[2] Jörg Hofmann,[1,6] Karl Seeger,[3] Detlev H. Krüger,[1] and Günther Schönrich[1]

[1]Institute of Medical Virology, Helmut-Ruska-Haus, [2]Department of Pediatric Pneumology and Immunology, and [3]Department of Pediatric Oncology and Hematology, Charité–Universitätsmedizin Berlin, 10117 Berlin, Germany
[4]Department of Nephrology, University of Heidelberg, 69120 Heidelberg, Germany
[5]Department of Dermatology and Allergic Diseases, University Hospital Ulm, 89081 Ulm, Germany
[6]Division of Virology, Labor Berlin Charité-Vivantes GmbH, 13353 Berlin, Germany

Rodent-borne hantaviruses are emerging human pathogens that cause severe human disease. The underlying mechanisms are not well understood, as hantaviruses replicate in endothelial and epithelial cells without causing any cytopathic effect. We demonstrate that hantaviruses strongly stimulated neutrophils to release neutrophil extracellular traps (NETs). Hantavirus infection induced high systemic levels of circulating NETs in patients and this systemic NET overflow was accompanied by production of autoantibodies to nuclear antigens. Analysis of the responsible mechanism using neutrophils from β2 null mice identified β2 integrin receptors as a master switch for NET induction. Further experiments suggested that β2 integrin receptors such as complement receptor 3 (CR3) and 4 (CR4) may act as novel hantavirus entry receptors. Using adenoviruses, we confirmed that viral interaction with β2 integrin induced strong NET formation. Collectively, β2 integrin–mediated systemic NET overflow is a novel viral mechanism of immunopathology that may be responsible for characteristic aspects of hantavirus-associated disease such as kidney and lung damage.

CORRESPONDENCE
Günther Schönrich:
guenther.schoenrich@charite.de

Abbreviations used: ANA, antinuclear antibody; CGD, chronic granulomatous disease; CR3, complement receptor 3; DAF, decay-accelerating factor; DPI, diphenyleneiodonium; dsDNA, double-stranded DNA; HTNV, Hantaan virus; LADIII, leukocyte adhesion deficiency type III; LFA-1, leukocyte function-associated antigen 1; MOI, multiplicity of infection; NADPH, nicotinamide adenine dinucleotide phosphate; NET, neutrophil extracellular trap; ROS, reactive oxygen species; SLE, systemic lupus erythematosus; VSV, vesicular stomatitis virus.

Neutrophils represent the most abundant cells of the immune system and account for 50–70% of circulating white blood cells in humans. As part of the first line of defense they play a crucial role in controlling invading pathogens (Borregaard, 2010). They eliminate bacteria by phagocytosis or by release of antimicrobial proteins during degranulation. Neutrophils can undergo a novel form of cell death program (Takei et al., 1996) which has been termed NETosis (Brinkmann et al., 2004). It results in the release of neutrophil extracellular traps (NETs), net-like structures of double-stranded DNA (dsDNA) coated with histones and antimicrobial molecules such as myeloperoxidase (Brinkmann et al., 2004). NETs not only capture and kill bacteria (Fuchs et al., 2007) but also have antiviral activity (Saitoh et al., 2012; Jenne et al., 2013).

In contrast, NET formation may cause immunopathology. NETs have recently been connected with various forms of autoimmune diseases including small-vessel vasculitis (Kessenbrock et al., 2009), psoriasis (Lin et al., 2011), rheumatoid arthritis (Khandpur et al., 2013), and systemic lupus erythematosus (SLE; Hakkim et al., 2010; Garcia-Romo et al., 2011; Lande et al., 2011; Villanueva et al., 2011). Thus, chromatin release during NET formation represents a source for autoantigens (Darrah and Andrade, 2012). If generated in the context of viral infections, NETs may be especially efficient in overcoming tolerance mechanisms and cause autoimmunity, as viruses induce the release of inflammatory cytokines such as type I IFN, a recognized contributing factor in SLE (Banchereau and Pascual, 2006).

How viruses induce NET formation is mostly unclear but signals emanating from viral entry receptors are likely to play a role. Many

P. Lalwani's present address is Infectious Diseases and Immunology Laboratory, Faculdade de Ciências Farmacêuticas, Universidade Federal do Amazonas, Manaus, AM, Brazil.

The Rockefeller University Press $30.00
J. Exp. Med. 2014 Vol. 211 No. 7 1485-1497
www.jem.org/cgi/doi/10.1084/jem.20131092

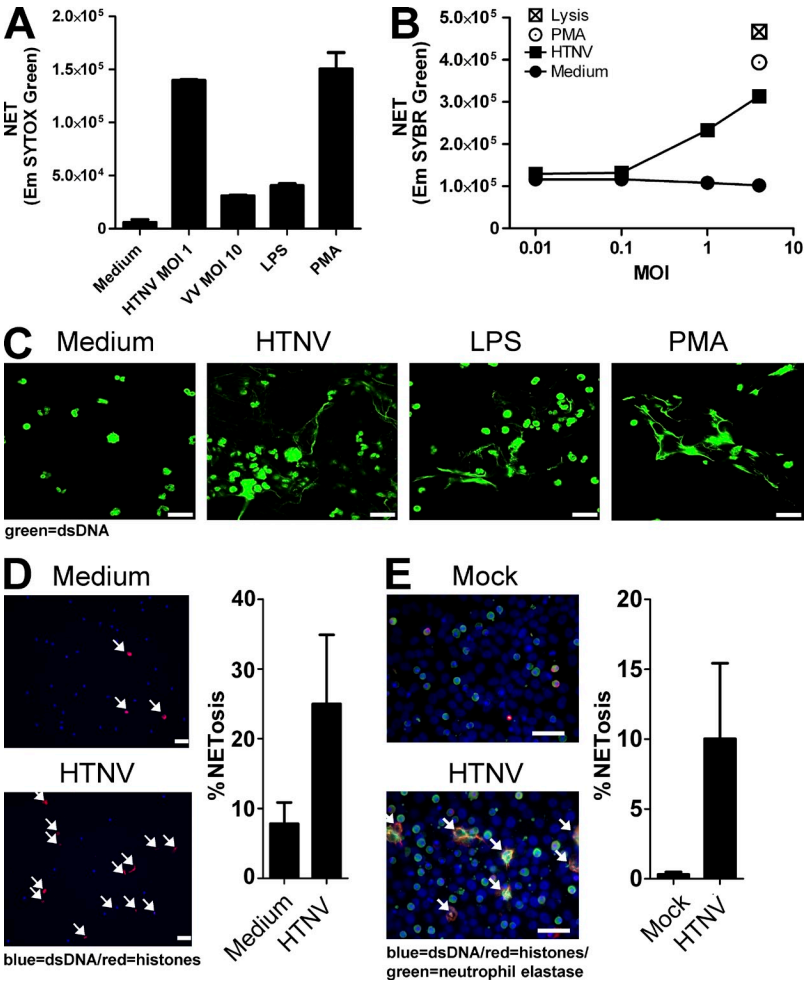

Figure 1. Virus-induced release of self-DNA from neutrophils in vitro. (A) Neutrophils were exposed to Hantaan virus (HTNV; multiplicity of infection [MOI] = 1), Vaccinia virus (VV; MOI = 10), 1 µg/ml LPS, or 100 nM PMA for 6 h. Neutrophils exposed to an equal volume of medium from uninfected Vero E6 cells (conditioned medium) served as a negative control. Subsequently, released self-DNA was stained with SYTOX Green, a cell-impermeable nucleic acid stain, and quantified. Neutrophils treated with LPS or PMA served as positive controls. Results shown are representative for three independent experiments done in triplicates. Error bars represent the mean ± SD. (B) Incubation of neutrophils with different MOIs of HTNV or PMA for 6 h. DNA release was measured by SYBR Green I staining of cell-free DNA compared with cells treated with an equal volume of conditioned medium. PMA-stimulated neutrophils and neutrophils lysed with Triton X-100 served as a maximal positive control. Results shown are representative of six independent experiments. (C) Confocal microscopy analysis of neutrophils incubated for 6 h with conditioned medium, HTNV (MOI = 1), LPS, or PMA before staining with SYTOX Green (bars, 20 µm). (D) Immunofluorescence analysis of neutrophils exposed to conditioned medium or HTNV (MOI = 1) for 4 h before staining with Bis-benzimide (Hoechst 33342, blue) and anti-histone antibody (red; bars, 50 µm). NET production (histone/Hoechst 33342 positivity, arrows) is shown as a percentage of total cell number in the right graph. (E) Immunofluorescence analysis of neutrophils exposed to monolayers of Vero E6 cells either mock-infected or infected with HTNV (MOI = 1). After 4 h, slides were stained with Hoechst 33342 (blue), an anti-histone antibody (red), and an antibody specific for neutrophil elastase (green; bars, 50 µm). NET production (NE/histone/DNA positivity, arrows) is shown as a percentage of total neutrophil number (right graph). In D and E, the mean values of 5 separate images were taken. Error bars represent the mean ± SD, and one representative experiment of two is shown.

nonenveloped and enveloped viruses use integrins, a large family of heterodimeric transmembrane proteins (Hynes, 2002), as receptors for attachment and/or cell entry (Stewart and Nemerow, 2007). During this process, viruses often trigger integrin signaling which alters various functions of the host cells. Integrins with a common β2 (CD18) chain are specifically expressed by leukocytes such as neutrophils. They represent key molecules that orchestrate neutrophil adhesion and transmigration across endothelial barriers (Ley et al., 2007). Genetically defective β2 integrin signaling in humans results in poor neutrophil function and recurrent bacterial infections, a disease called leukocyte adhesion deficiency. Intriguingly, β2 integrins also regulate neutrophil survival (Mayadas and Cullere, 2005; El Kebir and Filep, 2013). This suggests that viruses that target β2 integrins as receptor molecules for entry may profoundly influence the fate of neutrophils.

Here, we examined whether viruses that are known to interact with integrins trigger NET formation. Furthermore, we investigated whether NETs and autoantibodies are generated in patients infected with viruses that strongly stimulate integrin-dependent NETosis in vitro.

RESULTS

Hantaviruses strongly induce NETs in vitro

Hantaviruses are zoonotic pathogens that cause severe renal and pulmonary pathology in humans (Jonsson et al., 2010; Krüger et al., 2011). Hantaan virus (HTNV), the prototype member of the genus *Hantavirus*, stimulated NETosis of human neutrophils much more efficiently and at much lower titers than vaccinia virus or LPS (Fig. 1, A and B). PMA-stimulated or lysed human neutrophils served as maximal positive controls. By confocal microscopy analysis, extracellular dsDNA could be visualized in cultures of HTNV-exposed human neutrophils but not in human neutrophils exposed to conditioned medium which served as a negative control (Fig. 1 C). Significant NET production after exposure of human neutrophils to HTNV was also detected by quantitative immunofluorescence analysis (Fig. 1 D). In addition, NETosis was triggered by coculture of human neutrophils with HTNV-infected Vero E6 cells (Fig. 1 E). Besides HTNV, which is encountered in Asia, hantavirus strains endemic in Europe as well as New World hantaviruses also induced NETosis (unpublished data). In conclusion, hantaviruses are strong inducers of NET formation.

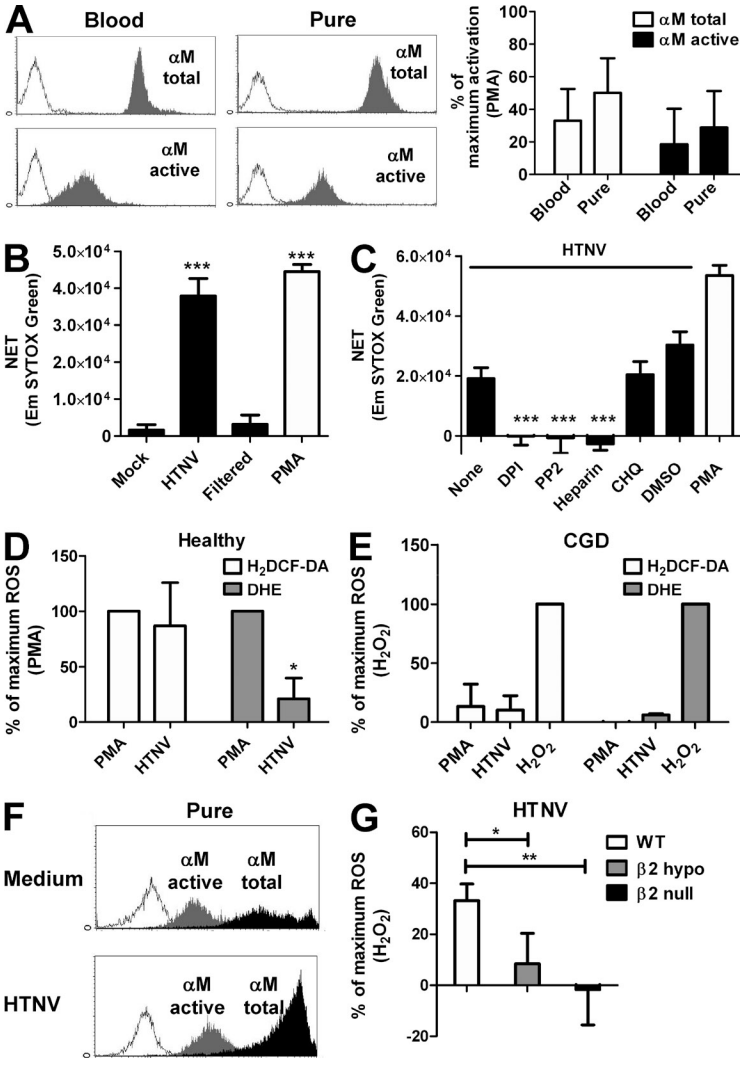

Figure 2. Src kinase inhibitor, NADPH oxidase inhibitor, and heparin abrogate hantavirus-induced NETosis. (A) Fresh blood samples and purified neutrophils were prepared from a single blood draw from three healthy human individuals. Subsequently, cells were stained with an antibody recognizing αM integrin irrespective of its activation status (αM total) or an antibody selectively reacting only with the activated form of αM integrin (αM active). A representative example of flow cytometric analysis is shown on the left side. The expression level of total αM and activated αM on blood neutrophils and purified neutrophils is given as percentage of maximal activation (PMA stimulation for 45 min) in the right graphs. Error bars represent the mean ± SD. Results from three independent experiments are shown. (B) Neutrophils from healthy human individuals were exposed for 6 h to supernatant from mock-infected or HTNV-infected (MOI = 1) Vero E6 cells, either unfiltered or filtered using a Viresolve Pro filter, or PMA. Released dsDNA was stained with SYTOX Green and quantified. Results shown are representative for three independent experiments done in triplicates. Error bars represent the mean ± SD. (C) Neutrophils from healthy human individuals were exposed to HTNV (MOI = 1; black bars) without pretreatment or after pretreatment with PP2, DPI, heparin, chloroquine (CHQ), or DMSO. Uninfected neutrophils treated with PMA served as a positive control (white bar). NETosis was determined by subtracting the SYTOX Green staining at 0 h from 6 h. Error bars represent the mean ± SD. Results shown are representative of four independent experiments done in triplicates. (D and E) Neutrophils from healthy human individuals (D) or CGD patients (E) were exposed to HTNV (MOI = 1) or stimulated with PMA or H_2O_2. After 6 h, neutrophils were stained with H_2DCF-DA or DHE and analyzed by flow cytometry. Results from four (D) or three (E) independent experiments using different donors are shown and are expressed as a percentage of maximum ROS production after stimulation with PMA (D) or H_2O_2 (E). Error bars represent the mean ± SEM. (F) Neutrophils from CGD patients exposed to supernatant from mock-infected (Medium) or HTNV-infected (MOI = 1) Vero E6 cells for 45 min were stained for the activated form of αM (gray filled-in curves) or total αM (black filled-in curves). Histograms shown are representative for three independent experiments. (G) Neutrophils from WT, β2 hypomorphic, and β2 null mice were exposed to HTNV (MOI = 1) for 8 h and subsequently stained with H_2DCF-DA. Data are shown as a percentage of maximum ROS production after stimulation of WT neutrophils with H_2O_2. Results from four independent experiments are shown. Error bars represent the mean ± SEM (***, $P < 0.001$; **, $P < 0.01$; *, $P < 0.05$; one-way ANOVA test with Bonferroni correction).

Hantavirus-induced NETosis requires viral particles, Src kinase signaling, and generation of reactive oxygen species (ROS)

We next determined the mechanism underlying HTNV-induced NETosis in human neutrophils. We excluded that the procedure used for neutrophil isolation resulted in significant activation by measuring expression of total integrin αM and active integrin αM (Fig. 2 A). Neither total integrin αM nor active integrin αM was significantly up-regulated on purified neutrophils as compared with untouched neutrophils in peripheral blood. The presence of viral particles was required for HTNV-induced NETosis (Fig. 2 B) but not prepriming with IFN-α or GM-CSF (not depicted). This suggested that a direct interaction of virions with cellular surface receptors plays an essential role. The compound diphenyleneiodonium (DPI), a known NETosis blocker (Fuchs et al., 2007), also prevented HTNV-induced NETosis (Fig. 2 C). DPI abrogates the activity of nicotinamide adenine dinucleotide phosphate (NADPH) oxidase, a multicomponent enzyme complex which generates antimicrobial ROS in response to invading pathogens. No inhibition was observed using chloroquine (Fig. 2 C), which interferes with endocytic TLR signaling (Häcker et al., 1998). The fact that chloroquine also prevents uncoating of hantaviral particles in the endolysosomal compartments indicated that viral replication is dispensable for hantavirus-induced NETosis. Hantavirus infection of neutrophils was nonproductive (unpublished data), further corroborating this point. Intriguingly, blocking Src kinases with PP2 impaired HTNV-triggered NETosis as efficiently as DPI (Fig. 2 C). Src kinases control downstream signaling of various cell surface receptors including integrins, which serve as receptors for pathogenic hantaviruses such as HTNV (Gavrilovskaya et al., 1998; Gavrilovskaya et al., 1999). In contrast, the non-integrin HTNV receptors decay-accelerating factor (DAF or CD55) and receptor for the globular head domain of complement (gC1qR)

were not involved. Their depletion by phosphatidylinositol-specific phospholipase C did not abolish HTNV-induced NET formation (unpublished data). Importantly, HTNV-induced NETosis was blocked by heparin (Fig. 2 C).

In accordance with a crucial role for NADPH oxidase in NETosis (Almyroudis et al., 2013), we observed that HTNV triggers ROS production in normal human neutrophils (Fig. 2 D). In contrast, neutrophils isolated from patients with chronic granulomatous disease (CGD), which have mutations in the NADPH oxidase gene (Babior, 1999), did not efficiently produce ROS after exposure to HTNV or PMA but responded normally to exogenous H_2O_2 (Fig. 2 E). Intriguingly, integrin αM (CD11b), which pairs with β2 integrin to form leukocyte-specific complement receptor 3 (CR3, also known as Mac-1), was activated by HTNV on neutrophils from CGD patients (Fig. 2 F). To establish if β2 integrin is involved in HTNV-triggered ROS production, we used neutrophils from genetically altered mice (Fig. 2 G). Neutrophils from β2 hypomorphic mice, which display strongly reduced β2 integrin levels (Wilson et al., 1993), generated only very low amounts of ROS in response to HTNV. Strikingly, neutrophils from β2 null mice, which are completely deficient in β2 expression (Scharffetter-Kochanek et al., 1998), were unable to produce ROS when stimulated with HTNV. Collectively, these results point to heparin-sensitive β2 integrin receptors being involved in hantavirus-induced generation of ROS and NETs.

β2 integrin mediates virus-induced NET formation

We next identified the heparin-sensitive integrin receptor responsible for NET induction after hantavirus infection. For this purpose, integrin expression on human neutrophils was examined (Fig. 3 A). β3 integrin, the known integrin receptor for pathogenic hantaviruses, was barely detectable on human neutrophils (Fig. 3 A) as compared with epithelial or endothelial cells (not depicted), which represent the major target cells of hantaviruses. This observation, together with the fact that heparin does not block entry of pathogenic hantavirus through β3 integrin (Gavrilovskaya et al., 1998), excluded the known integrin receptor for pathogenic hantaviruses. In contrast, β1 and β2 integrin were strongly expressed on human neutrophils (Fig. 3 A). Whereas β1 integrin is only a receptor for nonpathogenic hantaviruses (Gavrilovskaya et al., 1998), it is unknown if β2 integrin has any role in the context of hantavirus infection.

Indeed, antagonistic anti-β2 antibodies blocked NET formation induced by HTNV or PMA very efficiently (Fig. 3 B). Supporting the antibody-blocking data, neutrophils from β2 hypomorphic and β2 null mice did not undergo NETosis in response to HNTV (Fig. 3 C). They also reacted only poorly (β2 hypomorphic mice) or not at all (β2 null mice) to PMA, whereas their response to exogenously added H_2O_2 was comparable to that of WT mice (Fig. 3 C). Strikingly, neutrophils derived from a patient with leukocyte adhesion deficiency type III (LADIII), an extremely rare syndrome based on a mutated kindlin-3 which causes defective integrin signaling (Kuijpers et al., 2009), showed defective NETosis in response to HTNV (Fig. 3 D, left) that was associated with a lack of ROI induction (Fig. 3 D, middle). As expected, neutrophils from CGD patients generated NETs in response to exogenous H_2O_2 but not in response to HTNV or PMA (Fig. 3 D, right). The neutrophils from the LADIII patient were also 10–100× less sensitive to PMA (Fig. 3 E), which is known to activate β2 integrin by inside-out signaling (Hibbs et al., 1991). We further corroborated this finding by stimulating neutrophils from β2 hypomorphic and β2 null mice with different PMA concentrations (Fig. 3 F). Neutrophils from β2 hypomorphic mice produced fewer NETs and neutrophils from β2 null mice barely responded to PMA, whereas the response to exogenously added H_2O_2 was in the normal range. β2 hypomorphic and null mice were also refractory to PMA-induced loss of cytoskeletal F-actin which is a prominent feature of early stages of NETosis (Fig. 3 G).

We confirmed the importance of β2 integrin signaling for viral induction of NETosis using another experimental system. Adenovirus (Ad) type 2 (Ad2), the only adenovirus known to rely on β2 integrin as a coreceptor, strongly induced NETosis in human neutrophils, whereas adenoviruses using αvβ3 (Ad5), or non-integrin receptors (Ad12, Ad40, and Ad41), showed nugatory NET induction (Fig. 3 H). Collectively, these observations demonstrate a crucial role for β2 integrin in NETosis.

β2 integrins can serve as hantavirus entry receptors

The β2 integrin chain (CD18) noncovalently pairs not only with integrin αM (CD11b) to build CR3 (CD11b/CD18) but also with integrin αL (CD11a) and integrin αX (CD11c) to form leukocyte function-associated antigen 1 (LFA-1 or CD11a/CD18) and CR4 (or CD11c/CD18), respectively. Intriguingly, only two of the three β2 integrin receptors, i.e., CR3 and CR4, are heparin-sensitive (Diamond et al., 1995; Salas et al., 2000; Vorup-Jensen et al., 2005, 2007). This strongly suggested that one or both are involved in the HTNV-induced NETosis that is blocked in the presence of heparin. Thus, we next determined whether CR3 and CR4 can act as hantavirus entry receptors. For this purpose, we used CHO cells that express LFA-1, CR3, or CR4. As a control, we included CHO cells expressing αvβ3, the known integrin receptor for pathogenic hantaviruses. After exposure to HTNV, the HNTV N protein was detected in CHO-CR3 and CHO-CR4 cells as well as in CHO-αvβ3 cells, whereas CHO cells stably transfected with LFA-1 or empty vector (CHO-vector cells) remained negative (Fig. 4, A and B). As previously reported (Gavrilovskaya et al., 1998), CHO-αvβ3 cells remained infectable even in the presence of high heparin concentrations (Fig. 4 B). In striking contrast, HTNV infection of CHO-CR3 and CHO-CR4 cells was abrogated at low heparin concentrations (1 IU/ml).

In accordance with a role for CR3 and CR4 as hantavirus receptors, lentivirus pseudotyped with the envelope glycoproteins (Gc and Gn) of HTNV (HTNV pseudotype) transduced CHO-CR4 cells as efficiently as stably transfected CHO-$\alpha_v\beta_3$ cells and, to a lesser extent, CHO-CR3 cells, but

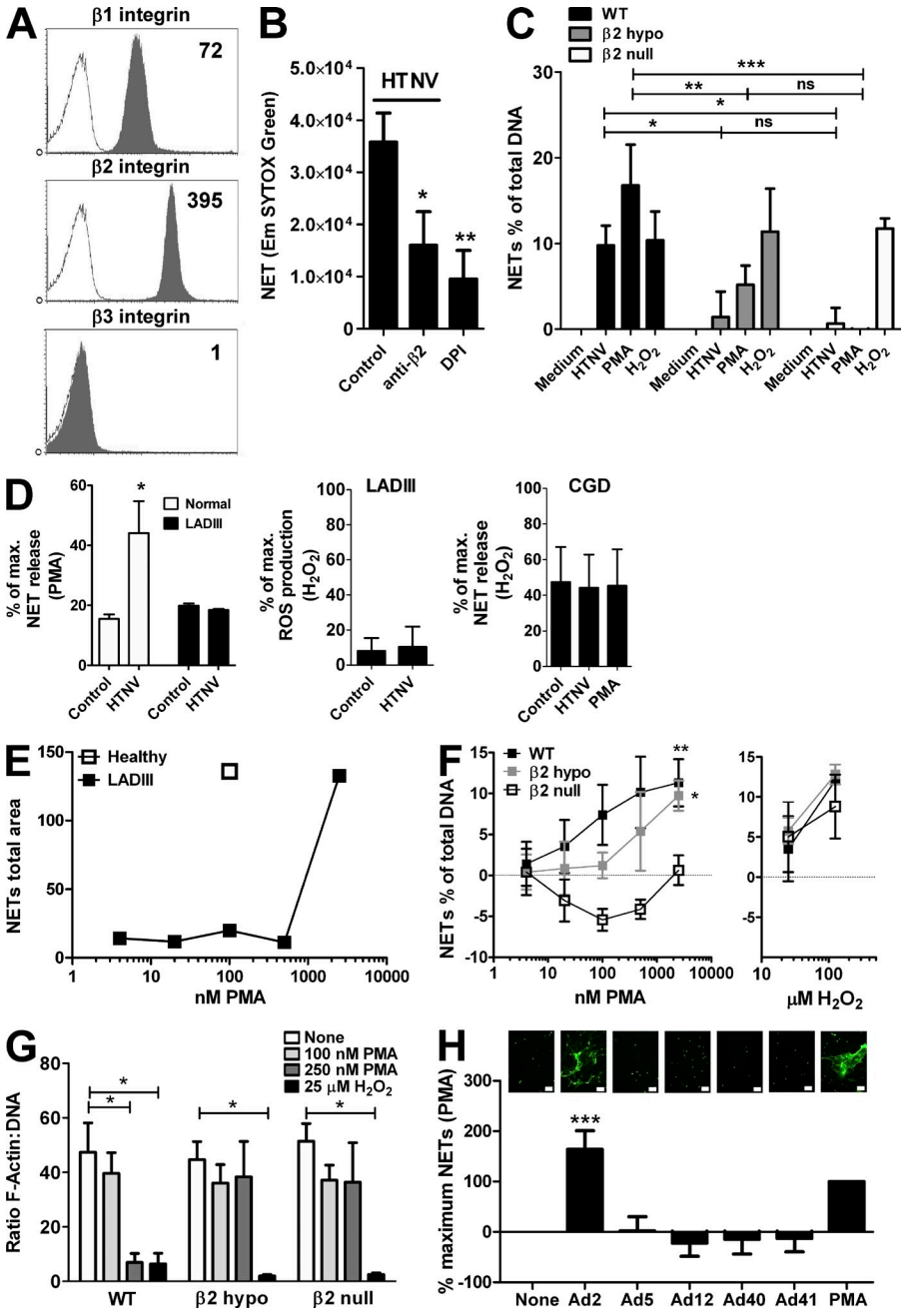

Figure 3. β2 integrin mediates virus-induced NETosis. (A) Neutrophils were stained for β1, β2, and β3 integrin. Representative flow cytometry histograms are shown and the specific mean fluorescence intensity is given in the top right corner. (B) Neutrophils were pretreated with control antibody, blocking anti-β2 antibody, or DPI before exposure to HTNV (MOI = 1) for 6 h and determination of NETosis by SYTOX Green staining. Error bars represent the mean ± SD (**, $P < 0.01$; *, $P < 0.05$). Results from three independent experiments are shown. (C) Neutrophils isolated from bone marrow of WT, β2 hypomorphic, or β2 null mice were exposed to conditioned medium or HTNV for 8 h or stimulated with 100 nM PMA or 25 μM H_2O_2 before quantifying NETosis by SYTOX Green staining. NET release is shown as a percentage of the total cellular DNA as determined by lysis with Triton X-100. Results from five independent experiments are shown. Error bars represent the mean ± SEM (***, $P < 0.001$; **, $P < 0.01$; *, $P < 0.05$; ns, not significant; one-way ANOVA test with Bonferroni correction). (D) Neutrophils from a healthy individual and a LADIII patient (left graph) and three CGD patients (right graph) were exposed to conditioned medium (control), HTNV (MOI = 1), or PMA. After 6 h, NETs were analyzed by Pico-Green staining of DNA released after digestion with micrococcal nuclease. NETosis is given as percentage of maximum NET release induced by PMA (left graph) or H_2O_2 (right graph); in neutrophils from the LADIII patient exposed to conditioned medium or HTNV, ROS production was additionally determined and is given as a percentage of maximum ROS production after stimulation of WT neutrophils with H_2O_2 (middle graph). Error bars represent the mean ± SEM (*, $P < 0.05$). (E) Neutrophils isolated from peripheral blood of a healthy individual and a LADIII patient were exposed to different quantities of PMA. After 6 h, NETs on coverslips were fixed and stained for DNA and histones as previously indicated. Results show the mean area of NETs of 5 random images as determined by ImageJ software. (F) Neutrophils isolated from bone marrow of WT, β2 hypomorphic, or β2 null mice were exposed to different quantities of PMA (left graph) or H_2O_2 (right graph) for 8 h before analysis by SYTOX Green staining. NET release is shown as a percentage of the total cellular DNA as determined by lysis with Triton X-100. Results from four independent experiments are shown. Error bars represent the mean ± SEM (**, $P < 0.01$; *, $P < 0.05$). (G) Murine neutrophils isolated from bone marrow of WT, β2 hypomorphic, or β2 null mice were exposed to different quantities of PMA or H_2O_2 for 1 h before analysis by cytometric staining with Phalloidin–Alexa Fluor 564 and DAPI for F-actin and DNA, respectively. Each slide was imaged 6 or more times and the ratio of F-actin to DNA was determined. The mean ratio of the images was then calculated. Results from 3–4 independent experiments are shown. Error bars represent the mean ± SEM (*, $P < 0.05$). (H) Neutrophils were exposed to different serotypes of adenovirus (MOI = 3). After 6 h, slides were fixed and stained with SYTOX Green. Total area staining for three randomly chosen images was determined using ImageJ software and the mean was calculated. Representative pictures are shown above the corresponding columns (bars, 50 μm). The results shown are derived from three independent experiments. Error bars represent the mean (relative to PMA) ± SD (***, $P < 0.001$; one-way ANOVA test with Bonferroni correction).

not CHO-vector cells (Fig. 4 C, top). In contrast, all transfected CHO cell lines were permissive for lentivirus pseudotyped with the vesicular stomatitis virus (VSV) G glycoprotein (VSV pseudotype; Fig. 4 C, bottom) orVSV infection (not depicted), which do not require integrin. Finally, UV-inactivated HTNV was able to trigger integrin signaling in CHO-CR3, CHO-CR4,

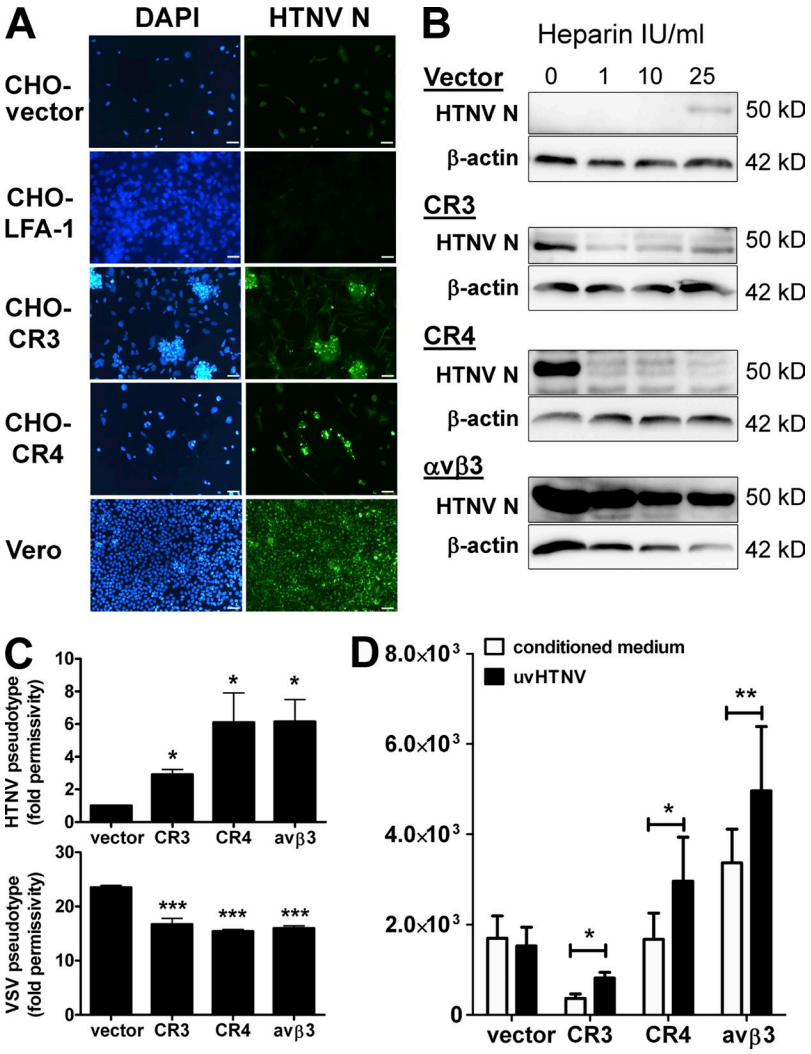

Figure 4. Identification of β2 integrin as a novel receptor for hantavirus infection. (A) Integrin-deficient CHO cells transfected with empty vector, LFA-1, CR3, or CR4 were infected for 4 d with HTNV (MOI = 1) and stained for hantavirus N protein by immunocytochemistry. Positive control is given by HTNV-infected Vero E6 cells (bars, 20 µm). (B) Integrin-deficient CHO cells transfected with empty vector, CR3, CR4, or αvβ3 as a positive control were left untreated or treated with increasing concentrations of heparin (IU/ml) before HTNV infection (MOI = 1). The results shown are representative for six independent experiments. (C) CHO cells as described for B were transduced by HTNV (top) or VSV (bottom) pseudotyped lentiviral vectors expressing GFP under the control of a constitutive promoter. After 3–5 d, the GFP expression was quantified. The fold permissivity to infection compared with infection of CHO-vector cells with HTNV pseudotype is given. The results shown are representative for five independent experiments done in triplicates. Error bars represent the mean ± SD. (D) CHO cells as described for B were transfected with a NF-κB reporter plasmid driving luciferase expression and a renilla expression plasmid driven by a constitutive promoter before being exposed to UV-inactivated hantavirus. Luciferase expression was measured relative to renilla expression. The results shown are representative of three independent experiments done in triplicates. Error bars represent the mean ± SD. ***, $P < 0.001$; **, $P < 0.01$; *, $P < 0.05$.

and CHO-$\alpha_v\beta_3$ cells but not in CHO-vector cells (Fig. 4 D). Collectively, these findings suggest that CR3 and CR4 are novel hantavirus entry receptors which are activated upon infection and mediate HTNV-induced NETosis.

Systemic NET overflow in hantavirus-infected patients

Having established by in vitro experiments that hantaviruses strongly induce NETosis through β2 integrin, we assessed NET formation in hantavirus-infected patients. NETs were detected in hantavirus-infected kidney biopsies (Fig. 5 A). In addition, strongly elevated levels of dsDNA (Fig. 5 B), circulating histone/dsDNA complexes (Fig. 5 C), and histone/myeloperoxidase complexes (not depicted) were found in sera from hantavirus-infected patients but not in healthy controls and patients with recent bacterial sepsis, influenza infection, or renal disease such as interstitial nephritis in the absence of hantavirus infection. The level of circulating histone/dsDNA complexes in hantavirus-infected patients was dependent on the disease stage (Fig. 5 D). In the acute phase of infection, 28% of patients showed increased levels of histone/dsDNA complexes rising to 53% in the convalescent phase. Intriguingly, the majority of patients still tested positive for blood histone/dsDNA complexes in the recovery phase. Moreover, patients with oliguria/polyuria had significantly higher levels of extracellular chromatin in the circulation (Fig. 5 E). Finally, patients infected with hantavirus strain PUUV had higher levels of circulating histone/dsDNA complexes than those infected with hantavirus strain DOBV (Fig. 5 F). DNase I activity was not impaired in sera from hantavirus-infected patients as compared with healthy controls (Fig. 5, G and H). This excludes changes in NET degradation as a possible cause of hantavirus-induced systemic NET overflow. Collectively, hantaviruses were found to generate high levels of NETs in vivo reflecting the strong NET-stimulatory capacity of hantaviruses in vitro.

Autoantibody production in response to virus-induced systemic NET overflow

We now determined whether the systemic NET overflow in hantavirus-infected patients was immunogenic. To this end, production of autoantibodies to nuclear antigens such as dsDNA and histones was determined. We observed antinuclear antibody (ANA) in sera from 32% of hantavirus-infected

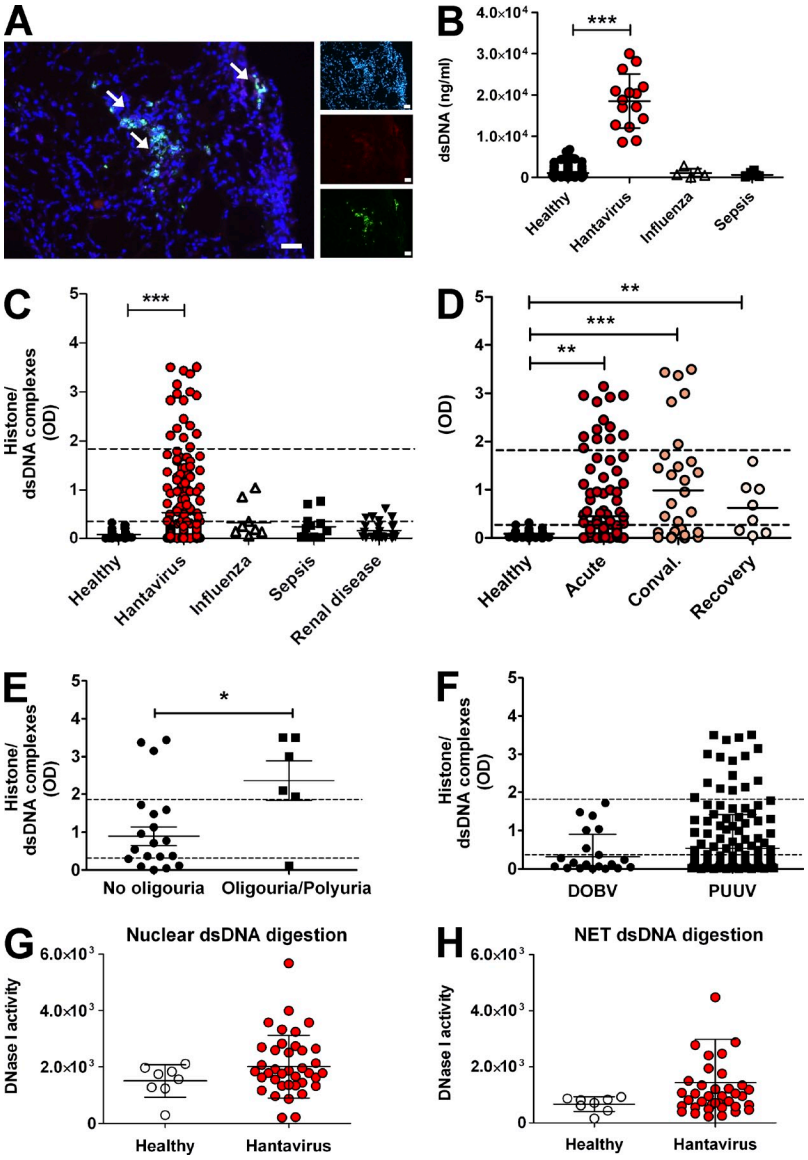

Figure 5. NETs and DNase I activity in hantavirus-infected patients. (A) Immunofluorescence analysis of renal biopsy from hantavirus-infected patient stained for DNA (blue), histones (red), and neutrophil elastase (green) as previously indicated (bars, 50 µm). Arrows show NET complexes (NE/histone/DNA positivity). Three out of four biopsies from four different patients were NET positive. All three control samples taken from healthy kidney tissue were negative. (B) The amount of dsDNA in serum probes from normal healthy individuals and infected patients was quantified by measuring the decrease in PicoGreen staining induced by an excess of DNase I. After a 5–8 h incubation with DNase I at 37°C, the reduction in PicoGreen staining was measured by using a fluorometer. Samples were calibrated by the same assay using known amounts of dsDNA. Error bars represent the mean ± SD. (C–F) Sera were examined by ELISA for the presence of circulating histone/dsDNA complexes. (C) Sera from healthy individuals, patients with active viral infections (hantavirus and influenza), or patients with bacterial sepsis or renal disease unrelated to hantavirus infection. (D) Hantavirus-infected patients in the acute, convalescent, or recovery phase. (E) Sera from hantavirus-infected patients with oliguria/polyuria and acute samples without oliguria/polyuria. Error bars represent the mean ± SEM. (F) Sera from patients infected with different hantavirus strains, DOBV (Dobrava-Belgrade virus), or PUUV (Puumala virus). The lower dotted lines correspond to the ELISA cutoff point, whereas the upper dotted lines show the sera from SLE patients as a positive control (***, $P < 0.0001$; **, $P < 0.01$; *, $P < 0.05$, Fisher's exact test, two-tailed). Error bars represent the mean ± SD. (G and H) Sera from healthy individuals and hantavirus-infected patients were tested for DNase I activity using dsDNA derived either from HEK 293 cells (G) or NETs (H). Error bars represent the mean ± SD.

patients (Fig. 6 A). Moreover, significantly increased levels of IgG antibodies to dsDNA were found in sera from hantavirus-infected patients but not from patients with influenza or bacterial sepsis (Fig. 6 B). In the recovery phase of hantavirus-associated disease autoantibody levels returned to normal (Fig. 6 C), although histone/dsDNA complexes were still present in many patients (Fig. 5 C). These data suggest that viral infection in general drives both NETosis as well as production of anti-dsDNA IgG antibodies.

DISCUSSION

We demonstrate here that β2 integrin serves as a viral pattern recognition receptor that stimulates systemic release of immunogenic self-DNA from neutrophils. The pathological relevance of this mechanism is supported by in vivo findings. NETs were detected in kidney biopsies and in sera from hantavirus-infected patients. Moreover, autoantibodies to nuclear antigens were produced that are usually associated with SLE, a disease connected to aberrant NET formation (Hakkim et al., 2010; Garcia-Romo et al., 2011; Lande et al., 2011; Villanueva et al., 2011).

We found that HTNV uses the β2 integrin receptors CR3 and CR4 as entry receptors and at the same time strongly induces both ROS production and NET formation through β2 integrin signaling. Consistent with these findings, enhanced ROS production has been detected in patients with hantavirus-associated disease (Davis et al., 2002). Emphasizing the relevance of β2 integrin receptors for virus-induced NET formation, we observed that Ad2, which uses β2 integrin as a coreceptor, but not β2 integrin–independent adenoviruses, also strongly stimulates NETosis. Moreover, CR3 is required for LPS-induced NETosis (Neeli et al., 2009). Others have observed that platelets that had been activated by gram-negative bacteria induce NETosis through LFA-1 (Yipp and Kubes, 2013). Altogether,

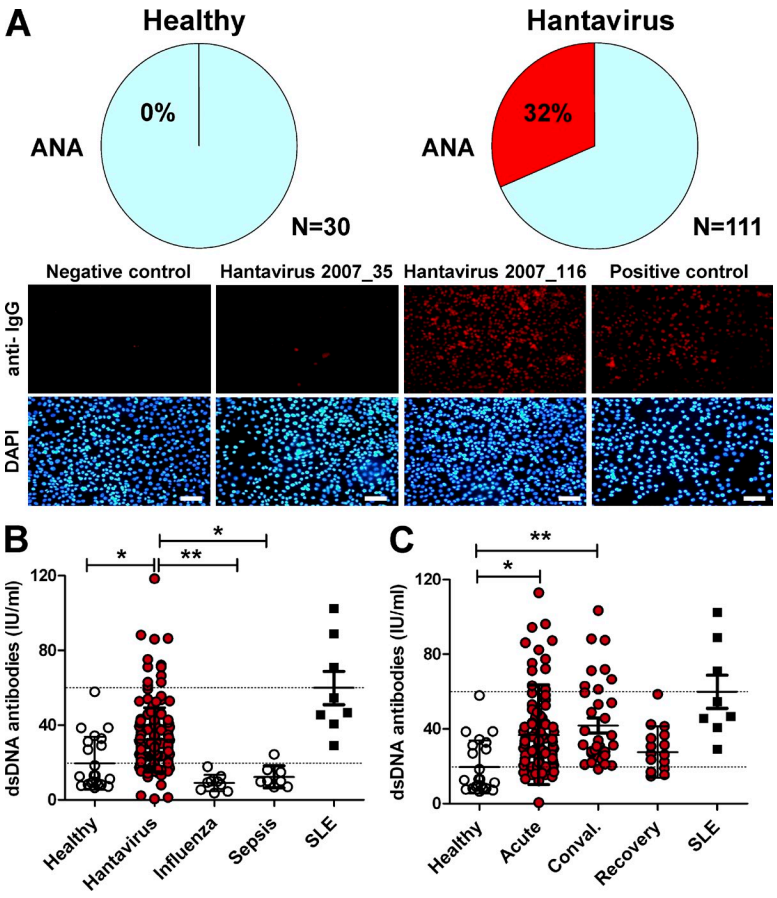

Figure 6. Elevated autoantibodies to nuclear antigens in virus-infected patients. Sera were analyzed for the level of autoantibodies. (A) For detection of ANAs, HEp-2 cells were fixed and permeabilized. Subsequently, cells were stained using a 1:180 dilution of serum followed by Texas red–coupled anti–human IgG (red) and DAPI (blue). Samples were taken as ANA-positive if clear nuclear staining was visible in comparison with a negative control (no serum). The top row shows pie charts that indicate the percentage of positive samples in sera from healthy individuals and hantavirus-infected patients, respectively. The bottom row shows as examples a serum from a negative control, from an ANA-negative and ANA-positive hantavirus-infected patient (2007_35 and 2007_116, respectively), and from a SLE patient used as a positive control (bars, 20 µm). (B and C) Anti-dsDNA IgG antibodies were determined by ELISA. The lower dotted lines correspond to the ELISA cut-off point, whereas upper dotted lines show the positive control, in this case sera from SLE patients. Error bars represent mean ± SD. **, $P < 0.01$; *, $P < 0.05$, one-way ANOVA test with Bonferroni correction.

these findings strongly imply that depending on the type of pathogen, different β2 integrin receptors on neutrophils play a crucial role in NETosis induction.

Underlining the importance of β2 integrin signaling for NETosis in general, we found that neutrophils from a LADIII patient with defective integrin signaling (Kuijpers et al., 2009) were 10–100× less sensitive to PMA-induced NETosis. Moreover, neutrophils from β2 hypomorphic and β2 null mice showed strongly impaired PMA-induced ROS production, F-actin loss, and NET formation. This suggests that in the absence of functional β2 integrin signaling, cytoskeletal rearrangement is blocked and neutrophils fail to actively extrude NETs. In contrast, binding of β2 integrin receptors to their natural ligands ICAM-1 or fibrinogen can increase neutrophil lifespan, and β2 integrin–mediated phagocytosis of complement-coated bacteria can lead to apoptosis (Mayadas and Cullere, 2005; El Kebir and Filep, 2013). Altogether, these findings indicate that the outcome of signaling through β2 integrins on neutrophils depends on the type of ligand and most likely on as yet unidentified additional signals. Thus, β2 integrin receptors represent a context-dependent master switch for NETosis.

It is known that β2 integrins as adhesive coreceptors are required for neutrophil responses triggered by a large number of stimuli such as TNF and other proinflammatory cytokines. Accordingly, TNF that is released by hantavirus-infected dendritic cells (Raftery et al., 2002; Marsac et al., 2011) and detectable in sera from hantavirus-infected patients (Linderholm et al., 1996) may act in concert with β2 integrins, thereby contributing to hantavirus-induced NETosis in vivo. It is possible that β2 integrins may allow adhesion-dependent activation triggered through hantavirus receptors other than β2 integrins. However, we did not find evidence for this scenario, as the absence of hantavirus non-integrin entry receptors on neutrophils, DAF, and gC1qR did not influence HNTV-induced NETosis (unpublished data). Moreover, the known integrin receptor for pathogenic hantavirus, β3 integrin, is not expressed by neutrophils. Nevertheless, the possibility that a yet unidentified hantavirus non-integrin receptor works upstream of β2 integrins cannot be categorically excluded.

We observed that viruses not known to use β2 integrins for entry such as vaccinia virus can also trigger NET formation, albeit at lower levels. This implies that common virus-sensing pattern recognition receptors such as TLRs can to some extent shift the fate of neutrophils toward NETosis. Consistent with this view, HIV-1 has recently been demonstrated to trigger NETosis by engagement of TLR7 and TLR8 (Saitoh et al., 2012). It is likely that the quantity and quality of virus-induced NET formation is determined not by single but rather by as-yet undefined virus-specific combinations of pattern recognition receptors. It remains to be analyzed how neutrophils "decide" to undergo NETosis in response to pathogens and in preference to other antimicrobial neutrophil

functions such as degranulation or phagocytosis, and if there is a special neutrophil subtype or maturation stage that is preferentially susceptible to virus-induced NETosis.

The strong NET-stimulatory capacity of hantaviruses we discovered may contribute to hantavirus-associated pathology in humans for several reasons. First, hantavirus infection of human endothelial cells does not cause a direct cytopathic effect (Pensiero et al., 1992; Temonen et al., 1993) but activates this cell type resulting in up-regulation of the β2 integrin ligand ICAM-1 (Temonen et al., 1996; Song et al., 1999; Geimonen et al., 2002). Upon interacting with activated endothelial cells neutrophils undergo NETosis (Gupta et al., 2010; Saffarzadeh et al., 2012), suggesting that hantavirus-infected endothelial cells are exposed to the deleterious effects of NETs in vivo. Second, activation of coagulation, which is observed in hantavirus-induced hemorrhagic fever (Lee et al., 1983), can also be a consequence of NETosis (Massberg et al., 2010). Moreover, besides human endothelial cells, hantaviruses infect human alveolar epithelial cells, which are damaged by NETs (Saffarzadeh et al., 2012). This contributes to the development of inflammatory lung tissue injury (Narasaraju et al., 2011), an important clinical feature of hantavirus-associated disease in humans (Rasmuson et al., 2011). Strongly supporting a role for NETs in hantavirus-associated immunopathology, we found high levels of circulating NETs in sera from hantavirus-infected patients but not from patients infected with other pathogens. These findings are consistent with the observation that cell-free DNA is regarded as an important biomarker of disease severity in hantavirus-infected patients (Outinen et al., 2012).

Virus-induced systemic NET overflow may have a strong impact on adaptive immune responses. First, NET-mediated priming of T cells (Tillack et al., 2012) may contribute to the vigorous antiviral T cell responses that are observed during human hantavirus infection (Kilpatrick et al., 2004; Manigold et al., 2010; Lindgren et al., 2011). Second, NETs cause the loss of tolerance to intracellular self-antigens, resulting in generation of autoantibodies to nuclear antigens (Sangaletti et al., 2012). In accordance with this report, we detected ANAs and elevated levels of IgG antibodies to dsDNA in sera from hantavirus-infected patients. Anti-dsDNA antibodies are thought to be highly specific for SLE and cause loss of kidney function (Tsokos, 2011), also a hallmark of hantavirus-associated disease. We also detected NETs in kidney biopsies from hantavirus-infected patients suggesting that NETs contribute to kidney damage. Direct proof that NETs induce kidney damage with signs of extracapillary glomerulonephritis and/or tubulointerstitial nephritis has recently been provided in a mouse model (Sangaletti et al., 2012).

We found that DNase I activity is not impaired in sera from hantavirus-infected patients excluding decreased NET degradation. Thus, hantavirus-induced NET formation is strong enough to overwhelm intact NET clearance mechanisms resulting in systemic NET overflow. In contrast, SLE patients show genetic polymorphisms associated with defective clearance of immune complexes (Tsokos, 2011). Accordingly, in SLE-prone individuals smaller quantities of NET-stimulatory viruses could induce systemic NET overflow. The latter might be more sustained and long-lasting, as humans are quite often subjected to apparent or inapparent infections with common viruses that may intermittently stimulate NET formation. This would explain why viral infections mimic SLE, induce SLE onset, or trigger lupus flares, a long-standing clinical observation (Ramos-Casals, 2008). Accordingly, the reported association between defective control of latent herpesvirus infection and SLE (Kang et al., 2004) may be due to increased and long-lasting viral replication driving NET formation.

Our results allow us to propose the following model of systemic NET excess development during infection and its contribution to pathology. NET overinduction through β2 integrin signaling overwhelms intact NET clearance mechanisms and results in systemic NET overflow. As a consequence, self-DNA becomes accessible to immune cells in the lymph nodes. There, self-reactive memory B cells are activated, most likely through coengagement of B cell receptor and TLR9 by self-DNA as demonstrated previously in animal experiments (Leadbetter et al., 2002). Type I IFN, the signature cytokine of viral infections, contributes to peripheral tolerance breakdown and activation and expansion of autoreactive B cells (Banchereau and Pascual, 2006). The resulting autoantibodies form immune complexes with NETs, which subsequently accumulate in the kidney and activate complement thereby causing damage. Supporting this notion, complement activation correlates with severity of hantavirus-associated disease (Lee et al., 1989; Paakkala et al., 2000). In addition, self-DNA may induce B cells to present antigen to nephrotoxic T cells that cause interstitial nephritis (Teichmann et al., 2013), a histopathological lesion frequently found in hantavirus-infected patients (Mustonen et al., 1994). On the basis of this concept, it appears possible that patients suffering from virus-induced systemic NET overflow could benefit from monitoring and therapeutic strategies aimed at NET formation.

MATERIALS AND METHODS

Viruses and infection. HTNV (strain 76–118; provided by Å. Lundkvist, Swedish Institute for Infectious Disease Control, Solna, Sweden), SNV (strain CC107; provided by P. Heinemann, Bernhard-Nocht-Institute for Tropical Medicine, Hamburg, Germany), DOBV (strain Slovenia; provided by T. Avšič-Županc, University of Ljubljana, Ljubljana, Slovenia), PUUV (strain Sotkamo; provided by A. Razanskiene, University of Vilnius, Vilnius, Lithuania), TULV (strain Lodz; provided by A. Plyusnin, University of Helsinki, Helsinki, Finland), or PHV (type 3571; provided by R.B. Tesh, University of Texas Medical Branch, Galveston, TX) were propagated on Vero E6 cells. Supernatant was collected from cell cultures 7–21 d after infection, cleared of cell debris by centrifugation at 2,000 *g*, aliquoted, and frozen at −80°C. Viral titer was ascertained as previously described (Heider et al., 2001). Other virus strains used were VSV Indiana (laboratory-adapted Mudd-Summers strain) and Vaccinia virus (Copenhagen strain). Adenoviruses were isolated from clinical samples and propagated on HEK 293 cells. Conditioned medium was generated from flasks of uninfected Vero E6 cells incubated for the same time as HTNV-infected flasks, and prepared as for infectious stocks.

For most assays granulocytes were not washed after exposure to virus. CHO cells were incubated with virus for 1 h at 37°C before being washed three times with PBS and incubated in the appropriate medium. Where relevant, cells were preincubated before infection for 30 min with blocking antibodies

to β2 (clone TS1/18; BioLegend) or isotype-matched control antibody (BD) at 10 µg/ml. The following reagents were used: PP2 (Merck) at 10 µM, DPI (Merck) at 10 µM, PMA (Sigma-Aldrich) at 100 nM, heparin (Sigma-Aldrich) at 10 µg/ml unless otherwise indicated, chloroquine (Sigma-Aldrich) at 2 mM, LPS (Sigma-Aldrich) at 1–10 µg/ml, and H_2O_2 (Merck) at 25 µM. GM-CSF and IFN-α 2a (ImmunoTools) were both used at 1,000 U/ml. Virus-containing supernatant was filtered by using a Viresolve Pro filter (Millipore), which yields a 4-log reduction in viral particles as small as 20 nm such as parvoviruses and is effective in removing HTNV virions (120 nm). All virus stocks and cells used were free of mycoplasma as tested by PCR-based VenorGeM mycoplasma detection kit (Minerva Biolabs). Mock infections were undertaken with conditioned medium prepared as for virus stocks except without infection.

Cell culture. Neutrophils were isolated from peripheral blood by centrifugation on discontinuous Percoll and Ficoll gradients (Aga et al., 2002) and cultivated in RPMI without phenol red but with 0.1% heat-inactivated FCS. Vero E6 cells were maintained in MEM (PAA) and CHO cells were cultured in Hams F12 medium (PAA) with nonessential amino acids and 4.5 g/liter glucose. These media were further supplemented with 10% FCS, 100 IU penicillin, 100 µg/ml streptomycin, and 4.5 mM L-glutamine. Neutrophils were resuspended in RPMI 1640 (PAA) without phenol red supplemented with 0.1% heat-inactivated FCS (BioWhittaker). Medium and FCS were certified endotoxin-free by the manufacturers. CHO-αvβ3 cells were supplied by I. Ahrens (University of Freiburg, Freiburg, Germany; Ahrens et al., 2006), and CHO-CR4, CHO-CR3, and CHO-vector cells were provided by D.T. Golenbock (University of Massachusetts Medical School, Worcester, MA; Medvedev et al., 1998).

Determination of NETosis. The induction of NETs was determined by immunocytochemistry and by quantifying the release of dsDNA as previously published (Brinkmann et al., 2004). For the latter, neutrophils (2×10^5 per well) exposed to virus stocks in flat-bottom 96-well plates were stained by SYTOX Green (Invitrogen), a cell-impermeable fluorescent DNA dye, according to the manufacturer's instructions. Alternatively, free dsDNA strands were generated by 10-min digestion with 1 U/ml micrococcal nuclease (Fermentas) before being stopped using 5 mM EDTA in PBS with 1% formaldehyde and stored at 4°C. The amount of dsDNA was subsequently estimated by SYBR Green (Invitrogen) or with PicoGreen (Invitrogen) staining. Quantification of dsDNA was performed on a luminometer (Mithras LB 940; Berthold Technologies). Specific NET formation was determined by subtracting the absorbance of neutrophils exposed for 0 h to virus from the value at 6 h. Immunocytochemistry was performed on samples fixed with formaldehyde (1–4%) for 24 h.

Quantification of dsDNA. Serum was diluted 1:10 with digestion buffer (PBS with 10 mM $MgSO_4$) and stained with PicoGreen (Invitrogen), an ultrasensitive fluorescent dsDNA stain, according to the manufacturer's instruction. Fluorescence was then measured using a Mithras (LB 940). An excess of DNase I (Invitrogen) was then added (1 U/sample) and the sample digested for 5–8 h. The intensity of PicoGreen staining (fluorescence emission) was determined every 2–3 h. To establish that digestion was complete and the DNase I was still active, the sample was spiked with 1 µg dsDNA (purified from HEK 293 cells) and the fluorescence intensity was again measured at time points 0, 5, and 12 h. By comparison with a dsDNA standard, the quantity of dsDNA present in samples was determined.

Bioassay for DNase I activity. Serum samples were diluted 1:50 with digestion buffer spiked with 1 µg/ml of dsDNA either from HEK 293 cells or NETs from PMA-stimulated granulocytes. Samples were stained with PicoGreen (Invitrogen) according to the manufacturer's instruction and incubated at 37°C. After a 5-h incubation at 37°C, the reduction in PicoGreen staining (fluorescence emission, Em) was measured using a fluorometer.

Flow cytometry and immunocytochemistry. For surface staining, cells were washed once with ice-cold wash solution (PBS with 1% heat inactivated FCS and 0.05% sodium azide) before being resuspended with the first antibody in ice-cold blocking solution (PBS with 10% heat-inactivated FCS and 0.2% sodium azide) for 1 h. The cells were then washed in ice-cold wash solution and the staining was repeated with FITC-coupled goat anti–mouse secondary antibody. After the final staining step, the cells were washed in ice-cold washing solution and then resuspended in 2 ml PBS with 1% formaldehyde. Flow cytometry was performed on a FACSCalibur (BD) and obtained results were analyzed using the software program CellQuest Pro (BD). For immunocytochemistry, cells were initially fixed with fresh paraformaldehyde 4% in PBS overnight. Slides were then washed three times in PBS, permeabilized with 0.5% Triton X-100 where relevant, and stained. Slides were examined either using a DMLB microscope (Leica) and a ProgRes camera (Jenoptik) with Capture Pro software (Kodak) or a DMR microscope (Leica) with Nuance spectral imaging system (PerkinElmer). Images were analyzed using the Fiji release of ImageJ software (National Institutes of Health). Confocal images were taken on a confocal system (LFSA; Leica) using LCS software (Leica).

Antibodies. For flow cytometry and immunocytochemistry, respectively, the following antibodies were used: anti-CD18 (anti–integrin β2; clone 6.7), anti-CD86 (clone IT2.2), anti-CD11b (anti–integrin αM; clone 44), and isotype-matched control antibodies (BD); anti-CD11c (anti–integrin αX; clone BU15), anti-CD61 (anti–integrin β3; clone C17), anti-CD29 (anti–integrin β1; clone MEM-101), and anti–GR-1 (clone RB6-8C5; ImmunoTools); anti-CD55/DAF (clone 143–30; Southern Biotechnology); anti-gC1qR (clone 74.5.2; EMD Millipore); anti-CD51 (anti–integrin αv; clone 13C2; QED Science, distributed by Acris Antibodies GmbH); and anti-histone (clone PL2-3) and anti-neutrophil elastase (clone 10D10) were produced in-house. Secondary antibodies coupled to fluorochrome or horseradish peroxidase were supplied by Dianova. Blocking antibody against CD18 (clone TS1/18) and antibody reacting with the activated form of αM integrin (clone CBRM1/5) were supplied by BioLegend. Hantavirus N protein was stained with N-specific polyclonal rabbit serum (Razanskiene et al., 2004). Anti–β-actin (clone ab6276) was purchased from Abcam.

ELISAs and detection of ANAs. The histone/dsDNA complexes were determined using Cell Death Detection ELISA^{PLUS} (Roche) according to the manufacturer's instructions and have been previously used as a NET-specific serum ELISA (Kessenbrock et al., 2009). For this assay, samples were diluted 1:10 in PBS. The ELISA for IgG antibodies to dsDNA was performed as previously described (Cohen and Maldonado, 2003) using dsDNA isolated from HEK 293 cells and treated with S1 nuclease to remove single-stranded DNA. The assay was validated using a commercially available ELISA for determination of IgG antibodies against dsDNA (IBL international). The ELISA for detection of histone-bound myeloperoxidase activity was performed as previously described (Kessenbrock et al., 2009).

ANA assays were performed by incubating fixed and permeabilized HEp-2 cells with serum from patients at different dilutions; data are shown at a dilution of 1:180. After washing, bound antibodies were visualized by staining with Texas red–conjugated affinity-purified anti-human IgG at a dilution of 1:400. Phalloidin–Alexa Fluor 564 (Invitrogen) was used at a dilution of 1:500 to determine F-actin.

Analysis of respiratory burst activity. The respiratory burst of neutrophils was analyzed in essence as described by others (Rothe and Valet, 1990). In brief, cells were stimulated with HTNV, PMA, or H_2O_2, a membrane-permeable oxidant. Subsequently, cells were treated for 30 min in the dark at 37°C with 2′,7′-dichlorodihydrofluorescein diacetate (H_2DCF-DA) or dihydroethidium (DHE), which were both provided by Molecular Probes and used at 5 µM. CM-H_2DCF-DA and DHE act as oxidation-sensitive fluorescent dyes that are used for detecting intracellular H_2O_2 and O_2^-, respectively. After treatment with H_2DCF-DA or DHE, cells were fixed and analyzed by flow cytometry.

Luciferase assay. Cells were plated out in 24-well plates at a density of 100,000 cells/well. Cells were transfected overnight with 200 ng NF-κB–driven

firefly luciferase plasmid (Agilent Technologies) and 20 ng of constitutively active renilla luciferase expression vector pRL-TK-Luc (Agilent Technologies) using PEI, with the medium being subsequently replaced with serum-free medium. Cells were then treated with UV-inactivated HTNV and lysed 24 h after transfection in 1× passive lysis buffer (Promega) by incubation for 15 min at 25°C with gentle agitation. Subsequently, firefly luciferase reporter activity was assayed and normalized to renilla luciferase activity. All luciferase assays were performed at least three times with similar results using the Dual-Luciferase Reporter Assay system (Promega) and a Mithras luminometer.

Lentivirus generation. Lentiviral vectors expressing GFP and pseudotyped for VSV-G or HTNV G proteins were generated using the third generation lentivirus system generated by D. Trono (Swiss Institutes of Technology, Zurich, Switzerland). Plasmid pcDNA3-GCP encoding HTNV envelope glycoprotein was provided by H. Feldmann (National Institute of Allergy and Infectious Diseases, Bethesda, MD). Transducing units were determined by serial dilution on Vero E6 cells and detection of GFP-expressing cells.

Blood samples. Blood samples were taken with informed consent and with approval from the ethical committee of the Charité–Universitätsmedizin Berlin. Serum samples were used throughout except for the bacterial sepsis patients where EDTA-plasma was used to reduce the chance of a false negative result. Acute hantavirus infection was defined as hantavirus-specific IgG titer being below IgM titer, convalescent patients were those with hantavirus-specific IgG titers above IgM titers but within 2 mo of initial presentation or disease symptoms, and recovered patients were patients 2 mo or more after diagnosis. Samples were collected in Germany from patients infected with TULV (Tula virus), PUUV (Puumala virus), or DOBV (Dobrava virus) harbored by the reservoir hosts *Microtus arvalis*, *Myodes glareolus*, and *Apodemus agrarius*, respectively. Hantavirus-specific IgM and IgG titers were determined by ELISA. Samples from patients showing signs of active infections, specifically influenza virus (IgA^+ or PCR^+) or bacterial sepsis (3–7 d after therapy), were taken for comparison. Control sera were derived from healthy individuals. The LADIII patient has a homozygous mutation in the *Fermt3* gene (*Kindlin3*) located in exon 12 (c.1525C>T) which results in a premature stop at codon 509 (p.Arg509X; Kuijpers et al., 2009).

Mice. Mice hypomorphic for integrin β2 expression (B6.129S7-*Itgb2*^{tm1Bay}/J; Wilson et al., 1993), β2 null mice (Scharffetter-Kochanek et al., 1998), and control C57BL/6J mice were obtained from Charles River and from a special pathogen-free breeding colony at the animal facility of the University Hospital Ulm, Germany. Granulocytes were isolated from bone marrow cells centrifuged over a discontinuous Percoll gradient for 30 min at 1,500 *g* as previously described (Ermert et al., 2009). Granulocytes were 86–92% pure as determined by GR-1 staining and flow cytometry. Granulocytes were treated to induce NET formation as for human cells, except for incubation for 8 h. NET formation was measured as for human neutrophils with SYTOX green staining. All animal experiments have been performed in accordance with institutional guidelines and have been approved by the Landesamt für Gesundheit und Soziales Berlin.

Statistical analysis. One-way ANOVA with Bonferroni correction was used throughout, apart from serum titer of dsDNA/histone complexes (Fig. 6, B and C) where Fisher's exact two-tailed Student's *t* test was used. Significance was assumed at $P < 0.05$. Statistical analysis was validated by the statistical department of the Charité–Universitätsmedizin.

We thank A. Zychlinsky and V. Brinkmann for helpful discussions, M. Bigalke and E. Lieske for excellent technical assistance, C. Priemer for cultivation of Vero E6 cells, S. Lepek for assisting in handling sera, and C. Goosmann for performing quantitative immunofluorescence analyses.

This work was supported by Deutsche Forschungsgemeinschaft (GraKo 1121 to P. Lalwani) and Charité—Universitätsmedizin Berlin (stipend to P. Lalwani).

The authors declare no competing financial interests.

Submitted: 26 May 2013
Accepted: 29 April 2014

REFERENCES

Aga, E., D.M. Katschinski, G. van Zandbergen, H. Laufs, B. Hansen, K. Müller, W. Solbach, and T. Laskay. 2002. Inhibition of the spontaneous apoptosis of neutrophil granulocytes by the intracellular parasite *Leishmania major*. *J. Immunol.* 169:898–905. http://dx.doi.org/10.4049/jimmunol.169.2.898

Ahrens, I.G., N. Moran, K. Aylward, G. Meade, M. Moser, D. Assefa, D.J. Fitzgerald, C. Bode, and K. Peter. 2006. Evidence for a differential functional regulation of the two β_3-integrins $\alpha_V\beta_3$ and $\alpha_{IIb}\beta_3$. *Exp. Cell Res.* 312:925–937. http://dx.doi.org/10.1016/j.yexcr.2005.11.036

Almyroudis, N.G., M.J. Grimm, B.A. Davidson, M. Röhm, C.F. Urban, and B.H. Segal. 2013. NETosis and NADPH oxidase: at the intersection of host defense, inflammation, and injury. *Front Immunol.* 4:45. http://dx.doi.org/10.3389/fimmu.2013.00045

Babior, B.M. 1999. NADPH oxidase: an update. *Blood*. 93:1464–1476.

Banchereau, J., and V. Pascual. 2006. Type I interferon in systemic lupus erythematosus and other autoimmune diseases. *Immunity*. 25:383–392. http://dx.doi.org/10.1016/j.immuni.2006.08.010

Borregaard, N. 2010. Neutrophils, from marrow to microbes. *Immunity*. 33:657–670. http://dx.doi.org/10.1016/j.immuni.2010.11.011

Brinkmann, V., U. Reichard, C. Goosmann, B. Fauler, Y. Uhlemann, D.S. Weiss, Y. Weinrauch, and A. Zychlinsky. 2004. Neutrophil extracellular traps kill bacteria. *Science*. 303:1532–1535. http://dx.doi.org/10.1126/science.1092385

Cohen, P.L., and M.A. Maldonado. 2003. Animal models for SLE. *Curr. Protoc. Immunol.* Chapter 15:Unit 15.20.

Darrah, E., and F. Andrade. 2012. NETs: the missing link between cell death and systemic autoimmune diseases? *Front Immunol*. 3:428.

Davis, I.C., A.J. Zajac, K.B. Nolte, J. Botten, B. Hjelle, and S. Matalon. 2002. Elevated generation of reactive oxygen/nitrogen species in hantavirus cardiopulmonary syndrome. *J. Virol.* 76:8347–8359. http://dx.doi.org/10.1128/JVI.76.16.8347-8359.2002

Diamond, M.S., R. Alon, C.A. Parkos, M.T. Quinn, and T.A. Springer. 1995. Heparin is an adhesive ligand for the leukocyte integrin Mac-1 (CD11b/CD1). *J. Cell Biol.* 130:1473–1482. http://dx.doi.org/10.1083/jcb.130.6.1473

El Kebir, D., and J.G. Filep. 2013. Modulation of neutrophil apoptosis and the resolution of inflammation through β2 integrins. *Front Immunol.* 4:60. http://dx.doi.org/10.3389/fimmu.2013.00060

Ermert, D., C.F. Urban, B. Laube, C. Goosmann, A. Zychlinsky, and V. Brinkmann. 2009. Mouse neutrophil extracellular traps in microbial infections. *J. Innate Immun.* 1:181–193. http://dx.doi.org/10.1159/000205281

Fuchs, T.A., U. Abed, C. Goosmann, R. Hurwitz, I. Schulze, V. Wahn, Y. Weinrauch, V. Brinkmann, and A. Zychlinsky. 2007. Novel cell death program leads to neutrophil extracellular traps. *J. Cell Biol.* 176:231–241. http://dx.doi.org/10.1083/jcb.200606027

Garcia-Romo, G.S., S. Caielli, B. Vega, J. Connolly, F. Allantaz, Z. Xu, M. Punaro, J. Baisch, C. Guiducci, R.L. Coffman, et al. 2011. Netting neutrophils are major inducers of type I IFN production in pediatric systemic lupus erythematosus. *Sci. Transl. Med.* 3:73ra20.

Gavrilovskaya, I.N., M. Shepley, R. Shaw, M.H. Ginsberg, and E.R. Mackow. 1998. β_3 Integrins mediate the cellular entry of hantaviruses that cause respiratory failure. *Proc. Natl. Acad. Sci. USA*. 95:7074–7079. http://dx.doi.org/10.1073/pnas.95.12.7074

Gavrilovskaya, I.N., E.J. Brown, M.H. Ginsberg, and E.R. Mackow. 1999. Cellular entry of hantaviruses which cause hemorrhagic fever with renal syndrome is mediated by β_3 integrins. *J. Virol.* 73:3951–3959.

Geimonen, E., S. Neff, T. Raymond, S.S. Kocer, I.N. Gavrilovskaya, and E.R. Mackow. 2002. Pathogenic and nonpathogenic hantaviruses differentially regulate endothelial cell responses. *Proc. Natl. Acad. Sci. USA*. 99:13837–13842. http://dx.doi.org/10.1073/pnas.192298899

Gupta, A.K., M.B. Joshi, M. Philippova, P. Erne, P. Hasler, S. Hahn, and T.J. Resink. 2010. Activated endothelial cells induce neutrophil extracellular traps and are susceptible to NETosis-mediated cell death. *FEBS Lett.* 584:3193–3197. http://dx.doi.org/10.1016/j.febslet.2010.06.006

Häcker, H., H. Mischak, T. Miethke, S. Liptay, R. Schmid, T. Sparwasser, K. Heeg, G.B. Lipford, and H. Wagner. 1998. CpG-DNA-specific activation of antigen-presenting cells requires stress kinase activity and is preceded by non-specific endocytosis and endosomal maturation. *EMBO J.* 17:6230–6240. http://dx.doi.org/10.1093/emboj/17.21.6230

Hakkim, A., B.G. Fürnrohr, K. Amann, B. Laube, U.A. Abed, V. Brinkmann, M. Herrmann, R.E. Voll, and A. Zychlinsky. 2010. Impairment of neutrophil

extracellular trap degradation is associated with lupus nephritis. *Proc. Natl. Acad. Sci. USA*. 107:9813–9818. http://dx.doi.org/10.1073/pnas.0909927107

Heider, H., B. Ziaja, C. Priemer, A. Lundkvist, J. Neyts, D.H. Krüger, and R. Ulrich. 2001. A chemiluminescence detection method of hantaviral antigens in neutralisation assays and inhibitor studies. *J. Virol. Methods*. 96:17–23. http://dx.doi.org/10.1016/S0166-0934(01)00314-7

Hibbs, M.L., S. Jakes, S.A. Stacker, R.W. Wallace, and T.A. Springer. 1991. The cytoplasmic domain of the integrin lymphocyte function-associated antigen 1 β subunit: sites required for binding to intercellular adhesion molecule 1 and the phorbol ester-stimulated phosphorylation site. *J. Exp. Med*. 174:1227–1238. http://dx.doi.org/10.1084/jem.174.5.1227

Hynes, R.O. 2002. Integrins: bidirectional, allosteric signaling machines. *Cell*. 110:673–687. http://dx.doi.org/10.1016/S0092-8674(02)00971-6

Jenne, C.N., C.H. Wong, F.J. Zemp, B. McDonald, M.M. Rahman, P.A. Forsyth, G. McFadden, and P. Kubes. 2013. Neutrophils recruited to sites of infection protect from virus challenge by releasing neutrophil extracellular traps. *Cell Host Microbe*. 13:169–180. http://dx.doi.org/10.1016/j.chom.2013.01.005

Jonsson, C.B., L.T. Figueiredo, and O. Vapalahti. 2010. A global perspective on hantavirus ecology, epidemiology, and disease. *Clin. Microbiol. Rev.* 23:412–441. http://dx.doi.org/10.1128/CMR.00062-09

Kang, I., T. Quan, H. Nolasco, S.H. Park, M.S. Hong, J. Crouch, E.G. Pamer, J.G. Howe, and J. Craft. 2004. Defective control of latent Epstein-Barr virus infection in systemic lupus erythematosus. *J. Immunol*. 172:1287–1294. http://dx.doi.org/10.4049/jimmunol.172.2.1287

Kessenbrock, K., M. Krumbholz, U. Schönermarck, W. Back, W.L. Gross, Z. Werb, H.J. Gröne, V. Brinkmann, and D.E. Jenne. 2009. Netting neutrophils in autoimmune small-vessel vasculitis. *Nat. Med*. 15:623–625. http://dx.doi.org/10.1038/nm.1959

Khandpur, R., C. Carmona-Rivera, A. Vivekanandan-Giri, A. Gizinski, S. Yalavarthi, J.S. Knight, S. Friday, S. Li, R.M. Patel, V. Subramanian, et al. 2013. NETs are a source of citrullinated autoantigens and stimulate inflammatory responses in rheumatoid arthritis. *Sci. Transl. Med*. 5:178ra40.

Kilpatrick, E.D., M. Terajima, F.T. Koster, M.D. Catalina, J. Cruz, and F.A. Ennis. 2004. Role of specific $CD8^+$ T cells in the severity of a fulminant zoonotic viral hemorrhagic fever, hantavirus pulmonary syndrome. *J. Immunol*. 172:3297–3304. http://dx.doi.org/10.4049/jimmunol.172.5.3297

Krüger, D.H., G. Schönrich, and B. Klempa. 2011. Human pathogenic hantaviruses and prevention of infection. *Hum. Vaccin*. 7:685–693. http://dx.doi.org/10.4161/hv.7.6.15197

Kuijpers, T.W., E. van de Vijver, M.A. Weterman, M. de Boer, A.T. Tool, T.K. van den Berg, M. Moser, M.E. Jakobs, K. Seeger, O. Sanal, et al. 2009. LAD-1/variant syndrome is caused by mutations in FERMT3. *Blood*. 113:4740–4746. http://dx.doi.org/10.1182/blood-2008-10-182154

Lande, R., D. Ganguly, V. Facchinetti, L. Frasca, C. Conrad, J. Gregorio, S. Meller, G. Chamilos, R. Sebasigari, V. Riccieri, et al. 2011. Neutrophils activate plasmacytoid dendritic cells by releasing self-DNA-peptide complexes in systemic lupus erythematosus. *Sci. Transl. Med*. 3:73ra19. http://dx.doi.org/10.1126/scitranslmed.3001180

Leadbetter, E.A., I.R. Rifkin, A.M. Hohlbaum, B.C. Beaudette, M.J. Shlomchik, and A. Marshak-Rothstein. 2002. Chromatin-IgG complexes activate B cells by dual engagement of IgM and Toll-like receptors. *Nature*. 416:603–607. http://dx.doi.org/10.1038/416603a

Lee, M., J.S. Lee, and B.K. Kim. 1983. Disseminated intravascular coagulation in Korean hemorrhagic fever. *Bibl. Haematol*. (49):181–199.

Lee, M., B.K. Kim, S. Kim, S. Park, J.S. Han, S.T. Kim, and J.S. Lee. 1989. Coagulopathy in hemorrhagic fever with renal syndrome (Korean hemorrhagic fever). *Rev. Infect. Dis.* 11:S877–S883. http://dx.doi.org/10.1093/clinids/11.Supplement_4.877

Ley, K., C. Laudanna, M.I. Cybulsky, and S. Nourshargh. 2007. Getting to the site of inflammation: the leukocyte adhesion cascade updated. *Nat. Rev. Immunol*. 7:678–689. http://dx.doi.org/10.1038/nri2156

Lin, A.M., C.J. Rubin, R. Khandpur, J.Y. Wang, M. Riblett, S. Yalavarthi, E.C. Villanueva, P. Shah, M.J. Kaplan, and A.T. Bruce. 2011. Mast cells and neutrophils release IL-17 through extracellular trap formation in psoriasis. *J. Immunol*. 187:490–500. http://dx.doi.org/10.4049/jimmunol.1100123

Linderholm, M., C. Ahlm, B. Settergren, A. Waage, and A. Tärnvik. 1996. Elevated plasma levels of tumor necrosis factor (TNF)-α, soluble TNF receptors, interleukin (IL)-6, and IL-10 in patients with hemorrhagic fever with renal syndrome. *J. Infect. Dis.* 173:38–43. http://dx.doi.org/10.1093/infdis/173.1.38

Lindgren, T., C. Ahlm, N. Mohamed, M. Evander, H.G. Ljunggren, and N.K. Björkström. 2011. Longitudinal analysis of the human T cell response during acute hantavirus infection. *J. Virol*. 85:10252–10260. http://dx.doi.org/10.1128/JVI.05548-11

Manigold, T., A. Mori, R. Graumann, E. Llop, V. Simon, M. Ferrés, F. Valdivieso, C. Castillo, B. Hjelle, and P. Vial. 2010. Highly differentiated, resting gn-specific memory $CD8^+$ T cells persist years after infection by andes hantavirus. *PLoS Pathog.* 6:e1000779. http://dx.doi.org/10.1371/journal.ppat.1000779

Marsac, D., S. García, A. Fournet, A. Aguirre, K. Pino, M. Ferres, A.M. Kalergis, M. Lopez-Lastra, and F. Veas. 2011. Infection of human monocyte-derived dendritic cells by ANDES Hantavirus enhances pro-inflammatory state, the secretion of active MMP-9 and indirectly enhances endothelial permeability. *Virol. J.* 8:223. http://dx.doi.org/10.1186/1743-422X-8-223

Massberg, S., L. Grahl, M.L. von Bruehl, D. Manukyan, S. Pfeiler, C. Goosmann, V. Brinkmann, M. Lorenz, K. Bidzhekov, A.B. Khandagale, et al. 2010. Reciprocal coupling of coagulation and innate immunity via neutrophil serine proteases. *Nat. Med*. 16:887–896. http://dx.doi.org/10.1038/nm.2184

Mayadas, T.N., and X. Cullere. 2005. Neutrophil β_2 integrins: moderators of life or death decisions. *Trends Immunol*. 26:388–395. http://dx.doi.org/10.1016/j.it.2005.05.002

Medvedev, A.E., T. Flo, R.R. Ingalls, D.T. Golenbock, G. Teti, S.N. Vogel, and T. Espevik. 1998. Involvement of CD14 and complement receptors CR3 and CR4 in nuclear factor-κB activation and TNF production induced by lipopolysaccharide and group B streptococcal cell walls. *J. Immunol*. 160:4535–4542.

Mustonen, J., H. Helin, K. Pietilä, M. Brummer-Korvenkontio, K. Hedman, A. Vaheri, and A. Pasternack. 1994. Renal biopsy findings and clinicopathologic correlations in nephropathia epidemica. *Clin. Nephrol*. 41:121–126.

Narasaraju, T., E. Yang, R.P. Samy, H.H. Ng, W.P. Poh, A.A. Liew, M.C. Phoon, N. van Rooijen, and V.T. Chow. 2011. Excessive neutrophils and neutrophil extracellular traps contribute to acute lung injury of influenza pneumonitis. *Am. J. Pathol*. 179:199–210. http://dx.doi.org/10.1016/j.ajpath.2011.03.013

Neeli, I., N. Dwivedi, S. Khan, and M. Radic. 2009. Regulation of extracellular chromatin release from neutrophils. *J. Innate Immun*. 1:194–201. http://dx.doi.org/10.1159/000206974

Outinen, T.K., T. Kuparinen, J. Jylhävä, S. Leppänen, J. Mustonen, S. Mäkelä, I. Pörsti, J. Syrjänen, A. Vaheri, and M. Hurme. 2012. Plasma cell-free DNA levels are elevated in acute Puumala hantavirus infection. *PLoS ONE*. 7:e31455. http://dx.doi.org/10.1371/journal.pone.0031455

Paakkala, A., J. Mustonen, M. Viander, H. Huhtala, and A. Pasternack. 2000. Complement activation in nephropathia epidemica caused by Puumala hantavirus. *Clin. Nephrol*. 53:424–431.

Pensiero, M.N., J.B. Sharefkin, C.W. Dieffenbach, and J. Hay. 1992. Hantaan virus infection of human endothelial cells. *J. Virol*. 66:5929–5936.

Raftery, M.J., A.A. Kraus, R. Ulrich, D.H. Krüger, and G. Schönrich. 2002. Hantavirus infection of dendritic cells. *J. Virol*. 76:10724–10733. http://dx.doi.org/10.1128/JVI.76.21.10724-10733.2002

Ramos-Casals, M. 2008. Viruses and lupus: the viral hypothesis. *Lupus*. 17:163–165. http://dx.doi.org/10.1177/0961203307086268

Rasmuson, J., C. Andersson, E. Norrman, M. Haney, M. Evander, and C. Ahlm. 2011. Time to revise the paradigm of hantavirus syndromes? Hantavirus pulmonary syndrome caused by European hantavirus. *Eur. J. Clin. Microbiol. Infect. Dis.* 30:685–690. http://dx.doi.org/10.1007/s10096-010-1141-6

Razanskiene, A., J. Schmidt, A. Geldmacher, A. Ritzi, M. Niedrig, A. Lundkvist, D.H. Krüger, H. Meisel, K. Sasnauskas, and R. Ulrich. 2004. High yields of stable and highly pure nucleocapsid proteins of different hantaviruses can be generated in the yeast Saccharomyces cerevisiae. *J. Biotechnol*. 111:319–333. http://dx.doi.org/10.1016/j.jbiotec.2004.04.010

Rothe, G., and G. Valet. 1990. Flow cytometric analysis of respiratory burst activity in phagocytes with hydroethidine and 2′,7′-dichlorofluorescin. *J. Leukoc. Biol*. 47:440–448.

Saffarzadeh, M., C. Juenemann, M.A. Queisser, G. Lochnit, G. Barreto, S.P. Galuska, J. Lohmeyer, and K.T. Preissner. 2012. Neutrophil extracellular

traps directly induce epithelial and endothelial cell death: a predominant role of histones. *PLoS ONE*. 7:e32366. http://dx.doi.org/10.1371/journal.pone.0032366

Saitoh, T., J. Komano, Y. Saitoh, T. Misawa, M. Takahama, T. Kozaki, T. Uehata, H. Iwasaki, H. Omori, S. Yamaoka, et al. 2012. Neutrophil extracellular traps mediate a host defense response to human immunodeficiency virus-1. *Cell Host Microbe*. 12:109–116. http://dx.doi.org/10.1016/j.chom.2012.05.015

Salas, A., M. Sans, A. Soriano, J.C. Reverter, D.C. Anderson, J.M. Piqué, and J. Panés. 2000. Heparin attenuates TNF-α induced inflammatory response through a CD11b dependent mechanism. *Gut*. 47:88–96. http://dx.doi.org/10.1136/gut.47.1.88

Sangaletti, S., C. Tripodo, C. Chiodoni, C. Guarnotta, B. Cappetti, P. Casalini, S. Piconese, M. Parenza, C. Guiducci, C. Vitali, and M.P. Colombo. 2012. Neutrophil extracellular traps mediate transfer of cytoplasmic neutrophil antigens to myeloid dendritic cells toward ANCA induction and associated autoimmunity. *Blood*. 120:3007–3018. http://dx.doi.org/10.1182/blood-2012-03-416156

Scharffetter-Kochanek, K., H. Lu, K. Norman, N. van Nood, F. Munoz, S. Grabbe, M. McArthur, I. Lorenzo, S. Kaplan, K. Ley, et al. 1998. Spontaneous skin ulceration and defective T cell function in CD18 null mice. *J. Exp. Med*. 188:119–131. http://dx.doi.org/10.1084/jem.188.1.119

Song, J.S., C.H. Min, E. Kang, and S.H. Yu. 1999. Expression of ICAM-1 on the Hantaan virus-infected human umbilical vein endothelial cells. *Korean J. Intern. Med*. 14:47–54.

Stewart, P.L., and G.R. Nemerow. 2007. Cell integrins: commonly used receptors for diverse viral pathogens. *Trends Microbiol*. 15:500–507. http://dx.doi.org/10.1016/j.tim.2007.10.001

Takei, H., A. Araki, H. Watanabe, A. Ichinose, and F. Sendo. 1996. Rapid killing of human neutrophils by the potent activator phorbol 12-myristate 13-acetate (PMA) accompanied by changes different from typical apoptosis or necrosis. *J. Leukoc. Biol*. 59:229–240.

Teichmann, L.L., D. Schenten, R. Medzhitov, M. Kashgarian, and M.J. Shlomchik. 2013. Signals via the adaptor MyD88 in B cells and DCs make distinct and synergistic contributions to immune activation and tissue damage in lupus. *Immunity*. 38:528–540. http://dx.doi.org/10.1016/j.immuni.2012.11.017

Temonen, M., O. Vapalahti, H. Holthöfer, M. Brummer-Korvenkontio, A. Vaheri, and H. Lankinen. 1993. Susceptibility of human cells to Puumala virus infection. *J. Gen. Virol*. 74:515–518. http://dx.doi.org/10.1099/0022-1317-74-3-515

Temonen, M., J. Mustonen, H. Helin, A. Pasternack, A. Vaheri, and H. Holthöfer. 1996. Cytokines, adhesion molecules, and cellular infiltration in nephropathia epidemica kidneys: an immunohistochemical study. *Clin. Immunol. Immunopathol*. 78:47–55. http://dx.doi.org/10.1006/clin.1996.0007

Tillack, K., P. Breiden, R. Martin, and M. Sospedra. 2012. T lymphocyte priming by neutrophil extracellular traps links innate and adaptive immune responses. *J. Immunol*. 188:3150–3159. http://dx.doi.org/10.4049/jimmunol.1103414

Tsokos, G.C. 2011. Systemic lupus erythematosus. *N. Engl. J. Med*. 365:2110–2121. http://dx.doi.org/10.1056/NEJMra1100359

Villanueva, E., S. Yalavarthi, C.C. Berthier, J.B. Hodgin, R. Khandpur, A.M. Lin, C.J. Rubin, W. Zhao, S.H. Olsen, M. Klinker, et al. 2011. Netting neutrophils induce endothelial damage, infiltrate tissues, and expose immunostimulatory molecules in systemic lupus erythematosus. *J. Immunol*. 187:538–552. http://dx.doi.org/10.4049/jimmunol.1100450

Vorup-Jensen, T., C.V. Carman, M. Shimaoka, P. Schuck, J. Svitel, and T.A. Springer. 2005. Exposure of acidic residues as a danger signal for recognition of fibrinogen and other macromolecules by integrin $\alpha_X\beta_2$. *Proc. Natl. Acad. Sci. USA*. 102:1614–1619. http://dx.doi.org/10.1073/pnas.0409057102

Vorup-Jensen, T., L. Chi, L.C. Gjelstrup, U.B. Jensen, C.A. Jewett, C. Xie, M. Shimaoka, R.J. Linhardt, and T.A. Springer. 2007. Binding between the integrin alphaXbeta2 (CD11c/CD18) and heparin. *J. Biol. Chem*. 282:30869–30877. http://dx.doi.org/10.1074/jbc.M706114200

Wilson, R.W., C.M. Ballantyne, C.W. Smith, C. Montgomery, A. Bradley, W.E. O'Brien, and A.L. Beaudet. 1993. Gene targeting yields a CD18-mutant mouse for study of inflammation. *J. Immunol*. 151:1571–1578.

Yipp, B.G., and P. Kubes. 2013. NETosis: how vital is it? *Blood*. 122:2784–2794. http://dx.doi.org/10.1182/blood-2013-04-457671